# Differential Diagnostic Value of Parathyroid 99mTc-MIBI SPECT/CT in MIBI Uptake Lesion

**Ri Sa**
The first Hospital of Jilin University
**Danyan Liu**
The First Hospital of Jilin University
**Sen Hou**
The First Hospital of Jilin University
**Hongguang Zhao**
The First Hospital of Jilin University
**Feng Guan** ( guanfeng1972@163.com )
The First Hospital of Jilin University

---

**Original research**

**Keywords:** MIBI, Parathyroid, PTH, Calcium, SPECT/CT

**Posted Date:** August 10th, 2020

**DOI:** https://doi.org/10.21203/rs.3.rs-54808/v1



---

# Abstract

**Background:** To investigate the role of parathyroid technetium-99m-hexakis2-methoxy-2-methylpropylisonitrile ($^{99m}$Tc-MIBI) single photon emission computed tomography/ computed tomography (SPECT/CT) combined with the serum calcium (Ca) and serum parathyroid hormone (PTH) in the differential diagnosis of MIBI uptake lesion.

**Methods:** 201 patients with MIBI uptake lesion on parathyroid $^{99m}$Tc-MIBI SPECT/CT from January 2015 to July 2019 were enrolled in this study. All patients who underwent surgical resection were classified into two groups: primary hyperparathyroidism (PHPT) and non-PHPT in terms of the pathological findings. Radiological performance of $^{99m}$Tc-MIBI SPECT/CT, serum Ca and serum PTH were comparable between the two groups.

**Results:** 201 patients (135 females; median age, 53.0 years; age range, 29 – 79 years) were included. Pathological findings were as follows: PHPT was in 126 (62.7%) patients, including parathyroid adenoma in 106 patients, parathyroid cancer in 12 patients and parathyroid hyperplasia in 8 patients, while non-PHPT were in 75 (37.3%) patients, including thyroid adenoma in 14 patients, thyroid papillary cancer in 15 patients and thyroid nodular goiter in 46 patients. In the following multivariable logistic regression analysis, serum Ca and diameter of the shortest axis of the lesion were the independent factors for differentiating PHPT from non-PHPT. In receiver operating characteristic (ROC) analyses, the cut-off value of serum Ca differentiating PHPT from non-PHPT was 2.6 mmol/L, yielding the area under the ROC curve (AUC) of 0.931, sensitivity of 85.7%, specificity of 89.2%; the cut-off value of diameter of the shortest axis of the lesion was 20.4mm, yielding AUC of 0.728, sensitivity of 62.2%, specificity of 87.1%.

**Conclusion:** Parathyroid $^{99m}$Tc-MIBI SPECT/CT combined with serum Ca and serum PTH contributed to the differential diagnosis of PHPT from non-PHPT, evenly can assist the determination of the specific pathology of MIBI uptake lesion before surgery.


# Background

Primary hyperparathyroidism (PHPT) is caused by a solitary parathyroid adenoma in 80% of cases, whereas four-gland hyperplasia accounts for 10–15%, multiple adenomas for 5% and parathyroid cancer for < 1% of cases [1]. It is characterized by hypercalcemia and elevated or inappropriately normal levels of parathyroid hormone (PTH) [2]. Parathyroid technetium-99m-hexakis2-methoxy-2-methylpropylisonitrile ($^{99m}$Tc-MIBI) single photon emission computed tomography/ computed tomography (SPECT/CT) is routinely used to assist the parathyroid surgeon in identifying the anatomic position of the abnormal gland(s) when planning parathyroidectomy [3].

However, the role of parathyroid $^{99m}$Tc-MIBI SPECT/CT in the qualitative diagnosis of MIBI uptake lesion remains indeterminate due to tracer accumulation of $^{99m}$Tc-MIBI is nonspecific. Normal parathyroid glands are not visible on $^{99m}$Tc-MIBI SPECT/CT, but hyper-functioning glands usually show increased radiopharmaceutical uptake. Unfortunately, many diseases not from parathyroid, show MIBI uptake, and cause false positive results. Diseases from thyroid such as thyroid nodular goiter, thyroid papillary cancer, thyroid follicular adenoma (oncocytic variant), and metastatic thyroid cancer were the main contributors for the false positive results [4]. Additionally, lymph nodes, branchial cleft remnants, and enlarged thymus acts with a cystic morphology also account for false positive results [5–7]. Currently, if there exists a suspicion of PHPT, parathyroid $^{99m}$Tc-MIBI SPECT/CT

would be performed for the location of hyper-functioning parathyroid lesion [8], and for the suspected PHPT, surgery would be carried out [9].

To date, it seems that determination of the nature of false positive lesion before the operation is out of duty of parathyroid $^{99m}$Tc-MIBI SPECT/CT, as this examination alone or combined use of serum Ca and serum PTH has not been used as a qualitative diagnosis of MIBI uptake lesion to provide abundant information of nature of the lesion. Actually, parathyroid $^{99m}$Tc-MIBI imaging followed by CT may provide many additional characteristics those were not valued in the past. We, therefore, conducted this study to evaluate the differential diagnostic role of parathyroid $^{99m}$Tc-MIBI SPECT/CT combined with serum Ca and serum PTH for the MIBI uptake lesion.

## Methods

# Patients

We conducted a retrospective review of consecutive patients with MIBI uptake lesion on preoperative parathyroid $^{99m}$Tc-MIBI SPECT/CT who subsequently underwent an operation and confirmed by pathological findings at our institution from January 2015 to July 2019. Serum Ca and serum PTH were performed in all patients before any treatments and after operation. Exclusion criteria were patients as follows: patients who were suspected with secondary hyperparathyroidism (SHPT); patients with multiple MIBI uptake lesions or ectopic parathyroid or ectopic thyroid; patients who had the history of parathyroid or thyroid surgery.

All patients provided informed written consent, which was ethically approved by the First Hospital of Jilin University research ethics committee.

### $^{99m}$ Tc-MIBI SPECT/CT

The dual-phase $^{99m}$Tc-MIBI examination consisted of an early phase SPECT and a delayed-phase SPECT/CT, which was obtained using dual-head SPECT/CT (GE Discovery NM/CT670). All patients were injected intravenously with 925–1110 MBq of $^{99m}$Tc-MIBI. Early phase SPECT images were obtained after 10 minutes and delayed-phase SPECT/CT images were acquired after 150 minutes with full views of the neck and thorax. Low-energy high-resolution collimators were used for image acquisition and images were acquired in a 128 × 128 matrix, with a 20% window centered around the voltage of 140 kV. A low-dose CT was registered immediately after SPECT without moving the patient for attenuation correction of SPECT images. CT slices (10 mm thick) were acquired in a 256 × 256 matrix, with 2.5 mA, 140 kV. Reconstruction was performed by the Ordered Subsets Expectation Maximization technique (OSEM). The images were inherently registered to Xeleris workstation software (GE Medical Systems).

# Image Interpretation

Two nuclear physicians who were unaware of the histopathological results interpreted all parathyroid $^{99m}$Tc-MIBI SPECT/CT findings by consensus. For visual analysis, a distinct focus of increased or separate MIBI uptake in the neck was considered positive for a PHPT on scintigraphy.

# Statistical Analysis

The continuous variables with non-normal distribution are presented as median (range). The categorical variables are reported as number (percentage). Comparisons of continuous variables between the two groups were performed with Mann-Whitney U-test and Kruskal-Wallis H-test were used in multiple groups. Categorical variables were compared by Pearson chi-square or Fisher's exact test as appropriate. Significant variables identified by univariate analyses were included in the subsequent multivariate logistic regression analysis. The optimum cut-off value of potential factors of differentiating PHPT from non-PHPT was calculated using receiver operating characteristic (ROC) curves. The area under the ROC curve (AUC) was calculated and used to compare the diagnostic value of these factors. Statistical analyses were performed using SPSS software (v. 24.0). All *p*-values were two-sided and $p < 0.05$ was considered statistically significant in all analyses.

## Results

# Patient Characteristics

A total of 243 patients with MIBI uptake lesion on parathyroid $^{99m}$Tc-MIBI SPECT/CT who underwent surgery were enrolled at the beginning. After exclusion of 46 patients (25 patients who were suspected with SHPT; 12 patients with multiple MIBI uptake lesions or ectopic parathyroid or ectopic thyroid; 5 patients who had the history of parathyroid or thyroid surgery), 201 patients (66 males, 135 females; median age, 53.0; age range, 29–79 years) were eligible for this study.

In terms of pathological findings, all enrolled subjects were classified into two groups: PHPT and non-PHPT. In detail, PHPT was in 126 (62.7%) patients, including parathyroid adenoma in 106 patients, parathyroid cancer in 12 patients, and parathyroid hyperplasia in 8 patients, while non-PHPT were in 75 (37.3%) patients, including thyroid adenoma in 14 patients, thyroid papillary cancer in 15 patients, and thyroid nodular goiter in 46 patients.

# Factors For Differentiating Phpt From Non-phpt

Upon analyzing the association of potential factors for differentiating PHPT from non-PHPT, a total of seven factors including age, gender, serum Ca, serum PTH, diameter of the shortest axis of the lesion, density, border of lesion was associated with differentiating PHPT from non-PHPT by univariate analysis.

In the following multivariable logistic regression analysis, serum Ca and diameter of the shortest axis of lesion were the independent factors for differentiating PHPT from non-PHPT (Table 1). In ROC analyses, the cut-off value of serum Ca was 2.6 mmol/L, yielding AUC of 0.931, sensitivity of 85.7%, specificity of 89.2%; the cut-off value of the diameter of the shortest axis of lesion was 20.4 mm, yielding AUC of 0.728, sensitivity of 62.2%, specificity of 87.1%.

Table 1
Comparison of potential factors associated with differential diagnosis of primary hyperparathyroidism from non-primary hyperparathyroidism patients (N = 201)

| Diagnosis | Univariate analysis | | | Multivariate analysis | | |
|---|---|---|---|---|---|---|
| | PHPT (n = 126) | non-PHPT (n = 75) | *P* | Odds ratio | 95% CI | *P* |
| Age (y) | 53.0 (32.0–79.0) | 53.0 (29.0–74.0) | 0.805 | 0.959 | 0.892–1.032 | 0.262 |
| Gender-n(%) | | | 0.000 | 0.429 | 0.073–2.528 | 0.350 |
| Male | 44 (34.9%) | 9 (12.0%) | | | | |
| Female | 82 (65.1%) | 66 (88.0%) | | | | |
| Serum PTH (pg/ml) | 299.4 (34.6–2140.0) | 100.0 (27.7–783.2) | 0.000 | 1.002 | 0.996–1.007 | 0.572 |
| Serum Ca (mmol/L) | 2.89 (2.24–5.70) | 2.24 (1.97–3.35) | 0.000 | 396.212 | 17.651–8893.68 | 0.000 |
| Diameter of the shortest axis (mm) | 12.8 (4.0–46.0) | 21.9 (3.4–51.6) | 0.000 | 0.891 | 0.826–0.962 | 0.003 |
| Density (Hu) | 41.0 (3.0–66.0) | 45.0 (25.0–105.0) | 0.008 | 0.955 | 0.892–1.021 | 0.176 |
| Border of the lesion-n(%) | | | 0.005 | 0.236 | 0.027–2.069 | 0.192 |
| Clear | 113 (89.7%) | 56 (74.7%) | | | | |
| Unclear | 13 (10.3%) | 19 (25.3%) | | | | |

PHPT, primary hyperparathyroidism; PTH, parathyroid hormone; Ca, calcium; CI, confidence interval.

### Factors Associated with Nature of Different Types of PHPT and Non-PHPT

In PHPT, serum Ca, serum PTH, and border of lesion were associated with the specific pathology (parathyroid adenoma, parathyroid cancer, parathyroid hyperplasia) (Table 2). The median serum PTH in parathyroid cancer was higher than those in the parathyroid adenoma and hyperplasia (both $p < 0.05$, $Z$=-1.399 and $Z$=-1.991). The median serum Ca in parathyroid adenoma was lower than those in the parathyroid cancer and parathyroid hyperplasia (both $p < 0.05$, $Z$=-3.131 and $Z$=-2.688). Lesion in parathyroid adenoma had clearer border than that in parathyroid cancer ($p < 0.05$, $Z$=-3.131). Representative casas of parathyroid adenoma, parathyroid cancer, and parathyroid hyperplasia on parathyroid $^{99m}$Tc-MIBI SPECT/CT are shown in Fig. 1–3.

Table 2
Comparison of patients regarding to the different pathology of primary hyperparathyroidism/non-primary hyperparathyroidism(N = 201)

| Diagnosis | PHPT (n = 126) | | | *P* | Non-PHPT (n = 75) | | | *P* |
|---|---|---|---|---|---|---|---|---|
| | parathyroid adenoma (n = 106) | parathyroid cancer (n = 12) | parathyroid hyperplasia (n = 8) | | thyroid adenoma (n = 14) | thyroid papillary cancer (n = 15) | thyroid nodular goiter (n = 46) | |
| Age (y) | 53.0 (32.0–79.0) | 46.0 (32.0–66.0) | 53.5 (32.0–66.0) | 0.528 | 53.0 (37.0–62.0) | 45.0 (34.0–74.0) | 54.0 (29.0–71.0) | 0.585 |
| Gender-n(%) | | | | 0.150 | | | | 0.042 |
| Male | 40 (37.7%) | 2 (16.7%) | 2 (25.0%) | | 0 (0%) | 5 (33.3%) | 4 (8.7%) | |
| Female | 66 (62.3%) | 10 (83.3%) | 6 (75.0%) | | 14 (100%) | 10 (67.7%) | 42 (91.3%) | |
| Serum PTH (pg/ml) | 201.3 (34.6–1602.5) | 821.7 (34.6–1602.5) | 324.8 (320.9–348.7) | 0.011 | 100.0 (34.9–178.1) | 45.3 (32.0–141.1) | 116.9 (27.7–783.2) | 0.267 |
| Serum Ca (mmol/L) | 2.81 (2.24–5.70) | 3.47 (3.19–3.72) | 3.16 (3.06–3.26) | 0.000 | 2.27 (2.07–2.58) | 2.24 (2.10–2.76) | 2.21 (1.97–3.35) | 0.764 |
| Radioactive uptake time-n(%) | | | | NS | | | | 0.002 |
| Early or delayed phase | 0 (0%) | 0 (0%) | 0 (0%) | | 0 (0%) | 3 (20.0%) | 0 (0%) | |
| Both phase | 106 (100%) | 12 (100%) | 8 (100%) | | 14 (100%) | 12 (80.0%) | 46 (100%) | |
| Radiation reduction of the lesion-n(%) | | | | NS | | | | 0.000 |
| Yes | 0 (0%) | 0 (0%) | 0 (0%) | | 14 (100%) | 15 (100%) | 21 (45.7%) | |
| No | 106 (100%) | 12 (100%) | 8 (100%) | | 0 (0%) | 0 (0%) | 25 (54.3%) | |
| Location correlated with thyroid-n(%) | | | | 0.072 | | | | 0.717 |
| Behind | 62 (58.5%) | 8 (66.7%) | 8 (100%) | | 2 (14.3%) | 1 (6.7%) | 6 (13.0%) | |
| In | 0 (0%) | 0 (0%) | 0 (0%) | | 12 (85.7%) | 14 (93.3%) | 38 (82.6%) | |
| Above | 6 (5.7%) | 0 (0%) | 0 (0%) | | 0 (0%) | 0 (0%) | 0 (0%) | |
| Below | 38 (35.8%) | 4 (33.3%) | 0 (0%) | | 0 (0%) | 0 (0%) | 2 (4.4%) | |

PHPT, primary hyperparathyroidism; PTH, parathyroid hormone; Ca, calcium.

| Diagnosis | PHPT (n = 126) | | | *P* | Non-PHPT (n = 75) | | | *P* |
|---|---|---|---|---|---|---|---|---|
| | parathyroid adenoma (n = 106) | parathyroid cancer (n = 12) | parathyroid hyperplasia (n = 8) | | thyroid adenoma (n = 14) | thyroid papillary cancer (n = 15) | thyroid nodular goiter (n = 46) | |
| Diameter of the shortest axis (mm) | 12.9 (4.0–46.0) | 12.8 (9.1–14.1) | 14.5 (10.9–24.8) | 0.881 | 27.3 (12.0–37.0) | 10.8 (3.4–21.0) | 22.1 (6.9–51.6) | 0.005 |
| Density (Hu) | 40.0 (3.0–66.0) | 44.0 (43.0–56.0) | 45.0 (16.0–46.0) | 0.215 | 46.0 (27.0–56.0) | 48.0 (36.0–76.0) | 44.0 (25.0–105.0) | 0.576 |
| Calcification-n(%) | | | | 0.999 | | | | 0.080 |
| Yes | 0 (0%) | 0 (0%) | 0 (0%) | | 4 (28.6%) | 0 (0%) | 6 (13.0%) | |
| No | 106 (100%) | 12 (100%) | 8 (100%) | | 10 (71.4%) | 15 (100%) | 40 (87.0%) | |
| Border of the lesion-n(%) | | | | 0.000 | | | | 0.013 |
| Clear | 100 (94.3%) | 6 (50%) | 7 (87.5%) | | 14 (100%) | 5 (33.3%) | 37 (80.4%) | |
| Unclear | 6 (5.7%) | 6 (50%) | 1 (12.5%) | | 0 (0%) | 10 (66.7%) | 9 (19.7%) | |

PHPT, primary hyperparathyroidism; PTH, parathyroid hormone; Ca, calcium.

In non-PHPT, gender, radioactive uptake time, radiation reduction of the lesion, the diameter of the shortest axis of lesion were associated with the specific pathology (thyroid adenoma, thyroid papillary cancer, thyroid nodular goiter) (Table 2). Lesion of thyroid nodular goiter was more likely to show radiation reduction in the center of the lesion than those in thyroid adenoma and thyroid papillary cancer (both $p < 0.05$, $Z$=-3.581, $Z$=-3.686). The median diameter of the shortest axis of lesion in thyroid papillary cancer was shorter than those of thyroid adenoma and thyroid nodular goiter (both $p < 0.05$, $Z$=-2.689, $Z$=-3.042). Similarly, lesion of thyroid papillary cancers were more likely to show unclear border than those of thyroid adenoma and thyroid nodular goiter (both $p < 0.05$, $Z$=-3.709, $Z$=-3.930). Comparing to thyroid papillary cancer, thyroid adenoma and thyroid nodular goiter more frequently occurred in female patient (both $p < 0.05$, $Z$=-2.333, $Z$=-2.317). Three cases showing MIBI uptake lesion only in the early phase were finally confirmed as thyroid cancers. Representative cases of thyroid adenoma, thyroid papillary cancer, and thyroid nodular goiter on parathyroid $^{99m}$Tc-MIBI SPECT/CT are shown in Fig. 4–6.

# Discussion

MIBI uptake lesion is used to be considered blindly as hyperparathyroidism since there is a lack of evidence for the role of differential diagnosis of parathyroid $^{99m}$Tc-MIBI SPECT/CT. For 201 patients with MIBI uptake lesion on parathyroid $^{99m}$Tc-MIBI SPECT/CT, approximately two-thirds of them were confirmed as PHPT, while one-third

of them were non-PHPT. This study demonstrated that parathyroid $^{99m}$Tc-MIBI SPECT/CT combined with serum Ca and serum PTH has potential qualitative diagnostic value for differentiating MIBI uptake lesion, which failed to be valued in the previous studies.

MIBI sensitivity is influenced by several factors. The study by Erbil Y et al [10] found that both adenoma weight and oxyphil cell content were significantly correlate with MIBI uptake. Especially adenoma weight > 600 mg, it is the most significant factor in obtaining MIBI uptake. MIBI deficiency glands are smaller than MIBI uptake glands. High oxyphil cell content (> 20%) is the an independent factor in obtaining MIBI uptake despite adenoma weight. The abundant intra-cytoplasmic mitochondria probably account for intense MIBI uptake by thyroid adenoma [11]. Furthermore, the cell cycle may play a role in imaging, where parathyroid cells are more likely to be in a G0 or non-growth phase while autonomous parathyroid tissues such as adenomas tend to be in a growth phase (G2 + S), which is common in SHPT [12]. Moreover, $^{99m}$Tc-MIBI scintigraphy is also related to preoperative serum Ca and serum PTH [13]. At last, autoimmune thyroid disease (AITD) is an important influential factor for MIBI uptake and may impede parathyroid lesion detection [4].

The first step for the management of MIBI uptake lesion on the parathyroid $^{99m}$Tc-MIBI SPECT/CT is to determine the origin of the lesion. By univariate analyses, gender, both serum Ca and serum PTH, the diameter of the shortest axis of the lesion, density, border of lesion were significant factors for differentiating PHPT from non-PHPT. PHPT is classically associated with an elevated level of total serum Ca and of serum PTH. However, in some patients, serum PTH level may be normal but inappropriate to hypercalcemia [1, 14]. In this study, we found similar findings by multivariate analyses, only serum Ca was independent factor for differentiating PHPT from non-PHPT. Lavryk OA et al [15] performed the extensive analysis of 1753 patients with PHPT, demonstrating 97% of them with either elevation of serum Ca or serum PTH, 20% with only elevation of serum PTH, and 6% with only elevation of serum Ca and 3% with both serum Ca and serum PTH within the reference range. Minimally elevated preoperative serum PTH levels can influence the management of PHPT [16]. However, in our study, the higher serum Ca is, the more PHPT likely to be (Table 1). The serum Ca, which is measured before receiving any treatments exerts relatively favorable value in differentiating PHPT from non-PHPT with the cut-off value of 2.6 mmol/L, yielding AUC of 0.931, sensitivity of 85.7%, specificity of 89.2%. The diameter of the shortest axis of the lesion is another independent factor for differentiating PHPT from non-PHPT. The diameter of shortest axis of non-PHPT is more likely larger than that of PHPT, with cut-off value of 20.4 mm, yielding AUC of 0.728, sensitivity of 62.2%, specificity of 87.1%.

SPECT/CT provides incremental value of the location of lesions [3, 17]. Definite location of the lesion would assist the ascertain nature of PHPT or non-PHPT. Most of the PHPT lesions locate behind the thyroid or below the thyroid, which can be clearly shown on the sagittal reconstruction on CT, while lesions from the thyroid are located in the thyroid.

The second question for the management of MIBI uptake lesion on the parathyroid $^{99m}$Tc-MIBI SPECT/CT is to determine the specific nature of PHPT or non-PHPT based on the radiological performance of $^{99m}$Tc-MIBI SPECT/CT combined with serum Ca and serum PTH. Parathyroid adenoma, parathyroid hyperplasia, parathyroid cancer are the main causes of the PHPT. Serum Ca, serum PTH, and border of lesion are significant factors for the differential diagnosis among them. Our study is in line with previous studies that the median serum PTH in parathyroid cancer is commonly much higher than serum PTH in other causes of PHPT, which would be 5 to 10 times higher than the upper limit of the norm [18]. The median serum Ca in parathyroid adenoma was lower than

those in parathyroid cancer and parathyroid hyperplasia. Not surprisingly, lesion of parathyroid cancers shows unclear border indicating infiltration of adjacent tissues.

In present study, the thyroid disease, such as thyroid nodular goiter, thyroid papillary cancer and thyroid adenoma greatly accounted for false positive results. Some features of non-PHPT still partially overlap with those of PHPT while some features on the $^{99m}$Tc-MIBI SPECT/CT is specifically for the non-PHPT, such as radiation reduction of the lesion and radioactive uptake time. Totally, in 21 patients, lesions with radiation reduction were confirmed as thyroid goiter nodular while in three patients, MIBI uptake lesions, which were visible only in the early phase were confirmed as thyroid papillary cancer. Based on our results, it is difficult to distinguish which phase is better for diagnosis of MIBI uptake lesion. However, according to Xue J et al [19] early scan of $^{99m}$Tc-MIBI SPECT/CT was much better than delayed scan. The diameter of the shortest axis of lesion and border of lesion play an important role in the determination of different types of non-PHPT. According to our results, larger lesions with clear border tend to be thyroid adenoma, which is full of eosinophilic cells. The border of lesion and relationship with surrounding tissues are efficiently in the distinction of malignancy lesions from benign ones. Thyroid papillary cancer commonly shows unclear rim and unevenly infiltrating the normal thyroid tissues around the lesion. On contrast, benign tumors, especially thyroid adenoma usually demonstrate clear border even if the diameter of the shortest axis of lesion is large.

We are fully aware that our study has several limitations: First, inherent limitations of a retrospective analysis and relatively small patient population of the parathyroid cancer, parathyroid hyperplasia, thyroid papillary cancer, thyroid adenoma could have affected the study results. In addition, $^{99m}$Tc-MIBI SPECT/CT characteristics were partially used to determine only single MIBI uptake lesion which was confirmed as PHPT. Multiple MIBI uptake lesions, ectopic thyroid lesion, ectopic parathyroid lesion and SPTH were excluded in our study. Furthermore, patients in our study refer to only six pathological types (parathyroid cancer, parathyroid hyperplasia, parathyroid hyperplasia, thyroid papillary cancer, thyroid adenoma, thyroid nodular goiter), some other diseases that may demonstrate MIBI uptake have not studied, which remains an area to explore for future studies.

# Conclusion

Parathyroid $^{99m}$Tc-MIBI SPECT/CT combined with serum Ca and serum PTH contributed to the differentiating PHPT from non-PHPT, evenly assisted the determination of the nature of MIBI uptake lesion to guide the further management.

# Abbreviations

$^{99m}$Tc-MIBI
technetium-99m-hexakis2-methoxy-2-methylpropylisonitrile; SPECT/CT:single photon emission computed tomography/ computed tomography; Ca:calcium; PTH:parathyroid hormone; PHPT:primary hyperparathyroidism; SHPT:secondary hyperparathyroidism; ROC:receiver operating characteristic curves; AUC:area under the ROC curve; AITD:autoimmune thyroid disease.

# Declarations

### Acknowledgements

Not applicable.

### Author's contributions

SR conceived and designed the study. SR, DL, SH, and GF contributed to the study design, enrolment of patients, and interpretation of the data. SR, SH, and GF analyzed and contributed to the interpretation of the data. SR drafted the report, and all authors edited and revised the report. All authors are responsible for the integrity of the data and accuracy of the analysis, and all approved the final report.

### Funding

None.

### Availability of data and materials

All data generated for this study are included in the manuscript.

### Ethics approval and consent to participate

The ethics board of The First Hospital of Jilin University approved the protocol and all subjects gave written informed consent for participation in the study.

### Consent for publication

Not applicable.

### Competing interests

The authors declare that they have no competing interests.

## References

1. Walker MD. Silverberg SJ. Primary hyperparathyroidism. Nat Rev Endocrinol. 2018;14:115–25.
2. Machado NN, Wilhelm SM. Diagnosis and Evaluation of Primary Hyperparathyroidism. Surg Clin North Am. 2019;99:649–66.
3. Prommegger R, Wimmer G, Profanter C, Sauper T, Sieb M, Kovacs P, et al. Virtual neck exploration: a new method for localizing abnormal parathyroid glands. Ann Surg. 2009;250:761–5.
4. Boi F, Lombardo C, Cocco MC, Piga M, Serra A, Lai ML, et al. Thyroid diseases cause mismatch between MIBI scan and neck ultrasound in the diagnosis of hyperfunctioning parathyroids: usefulness of FNA-PTH assay. Eur J Endocrinol. 2013;168:49–58.
5. Lee H, Gault CR, Cheng G, Shah JC, Pantel AR. 99mTc-MIBI Uptake in a Benign Thymic Cyst. Clin Nucl Med. 2019;44:150–2.
6. Leslie WD, Riese KT, Mohamed C. Sestamibi retention in reactive lymph node hyperplasia: a cause of false-positive parathyroid localization. Clin Nucl Med. 2000;25:216–7.

7. Zhang J. Mediastinal Remnant Thymic Tissue Misdiagnosed as Ectopic Parathyroid Hyperplasia in Secondary Hyperparathyroidism. Clin Nucl Med. 2018;43:943–5.
8. Bahador FM, Latifi HR, Grossman SJ, Oza UD, Xu H. Griffeth LK. Optimal interpretative strategy for preoperative parathyroid scintigraphy. Clin Nucl Med. 2015;40:116–22.
9. Pallan S, Rahman MO, Khan AA. Diagnosis and management of primary hyperparathyroidism. Bmj. 2012;344:e1013.
10. Erbil Y, Kapran Y, Issever H, Barbaros U, Adalet I, Dizdaroglu F, et al. The positive effect of adenoma weight and oxyphil cell content on preoperative localization with 99mTc-sestamibi scanning for primary hyperparathyroidism. Am J Surg. 2008;195:34–9.
11. Strauss HW. MIBI and mitochondria. J Am Coll Cardiol. 2013;61:2018–9.
12. Rubello D, Fanti S, Nanni C, Farsad M, Castellucci P, Boschi S, et al. 11C-methionine PET/CT in 99mTc-sestamibi-negative hyperparathyroidism in patients with renal failure on chronic haemodialysis. Eur J Nucl Med Mol Imaging. 2006;33:453–9.
13. Cordes M, Dworak O, Papadopoulos T, Coerper S, Kuwert T. MIBI scintigraphy of parathyroid adenomas: correlation with biochemical and histological markers. Endocr Res. 2018;43:141–8.
14. Hindie E, Zanotti-Fregonara P, Tabarin A, Rubello D, Morelec I, Wagner T, et al. The role of radionuclide imaging in the surgical management of primary hyperparathyroidism. J Nucl Med. 2015;56:737–44.
15. Lavryk OA, Siperstein AE. Use of Calcium and Parathyroid Hormone Nomogram to Distinguish Between Atypical Primary Hyperparathyroidism and Normal Patients. World J Surg. 2017;41:122–8.
16. Bilezikian JP, Bandeira L, Khan A, Cusano NE, Hyperparathyroidism. Lancet. 2018;391:168–78.
17. Mahajan S, Schoder H. Ectopic Undescended Parathyroid Adenoma-SPECT/CT Avoids False-Negative Interpretation on 99mTc-MIBI Dual-Phase Scintigraphy. Clin Nucl Med. 2018;43:199–200.
18. Machado NN, Wilhelm SM. Parathyroid Cancer: A Review. Cancers (Basel). 2019;11.
19. Xue J, Liu Y, Yang D, Yu Y, Geng Q, Ji T, et al. Dual-phase 99mTc-MIBI imaging and the expressions of P-gp, GST-pi, and MRP1 in hyperparathyroidism. Nucl Med Commun. 2017;38:868–74.

# Figures

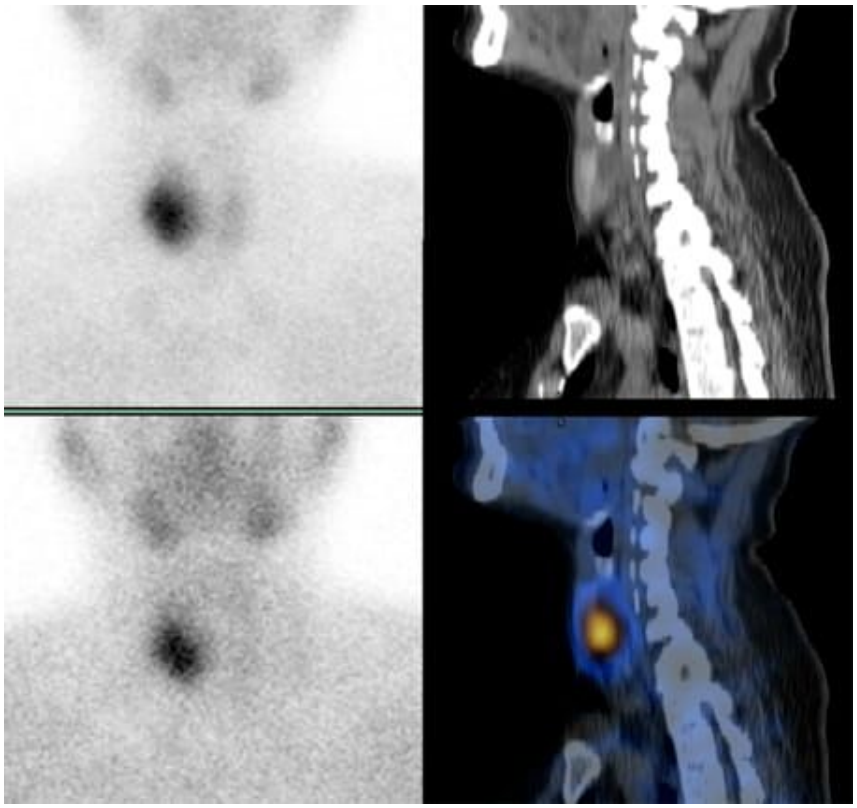

**Figure 1**

A 63-year-old male patient of parathyroid adenoma with serum Ca 2.76mmol/L and serum PTH 462.9pg/ml. Parathyroid 99mTc-MIBI SPECT/CT showed MIBI uptake lesion, which was located behind the thyroid possessing low density and clear border.

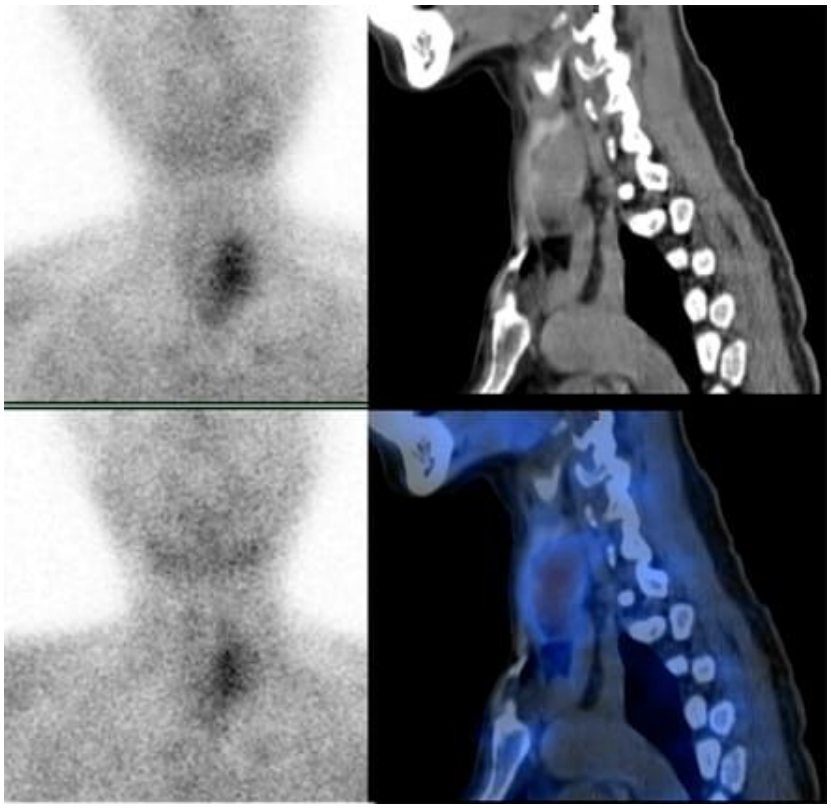

**Figure 2**

A 66-year-old female patient of parathyroid cancer with serum Ca 3.45mmol/L and serum PTH 1312.5pg/ml. Parathyroid 99mTc-MIBI SPECT/CT showed MIBI, which was behind the thyroid infiltrating to surrounding thyroid tissue.

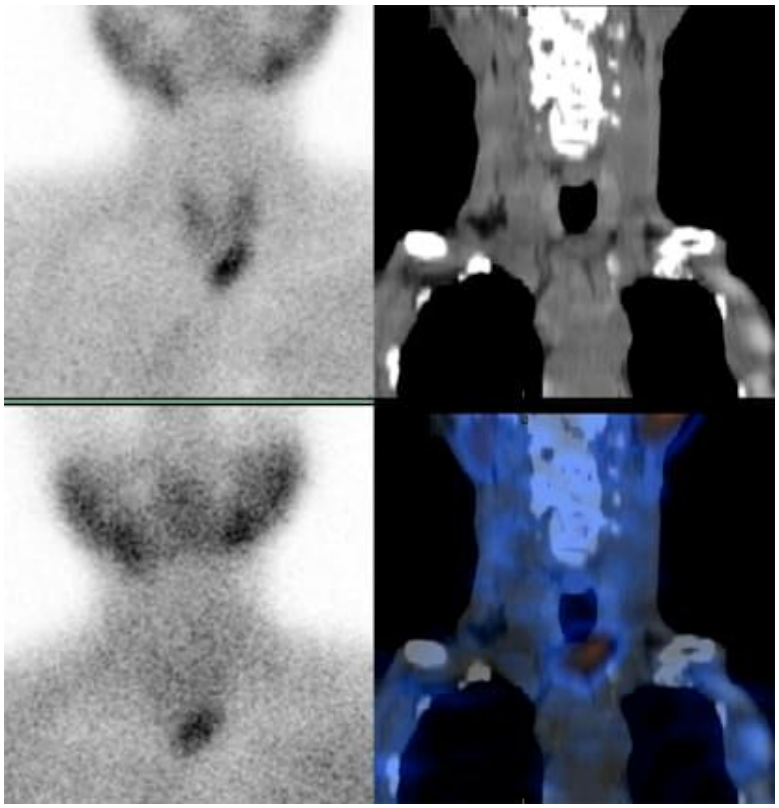

**Figure 3**

A 64-year-old male patient of parathyroid hyperplasia with serum Ca 3.26mmol/L and serum PTH 324.8pg/ml. Parathyroid 99mTc-MIBI SPECT/CT showed MIBI uptake lesion, which was located below the thyroid possessing low density and clear border.

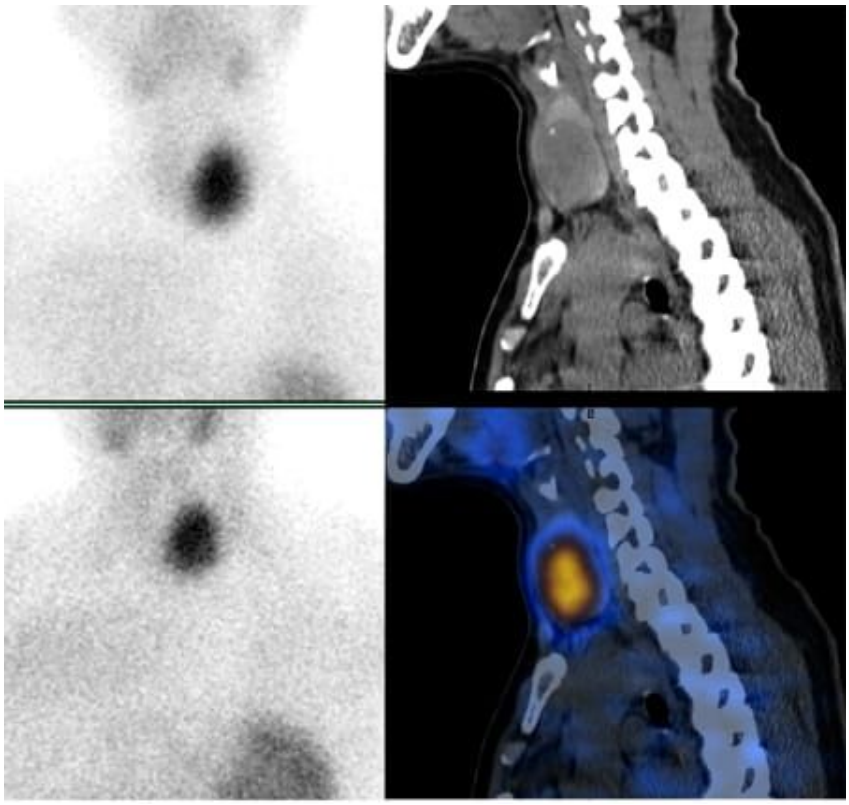

**Figure 4**

A 37-year-old female patient of thyroid adenoma with serum Ca 2.25mmol/L and serum PTH 37.5pg/ml. Parathyroid 99mTc-MIBI SPECT/CT showed MIBI uptake lesion, which was located in the thyroid.

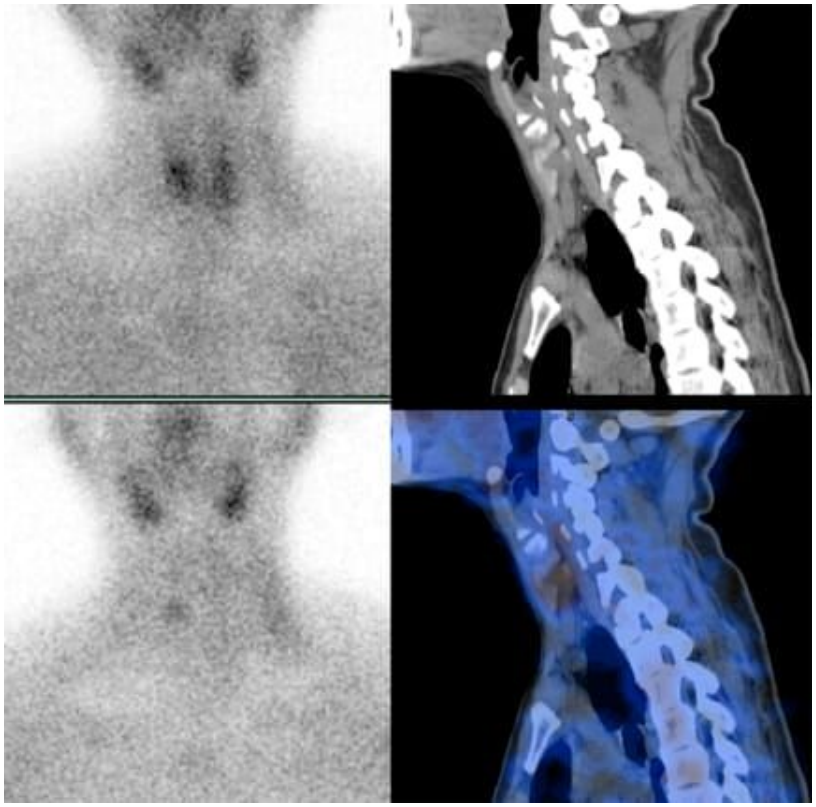

**Figure 5**

A 41-year-old female patient of thyroid papillary cancer with serum Ca 2.19mmol/L and serum PTH 45.3pg/ml. Parathyroid 99mTc-MIBI SPECT/CT showed MIBI uptake lesion, which was located in the thyroid possessing unclear border.

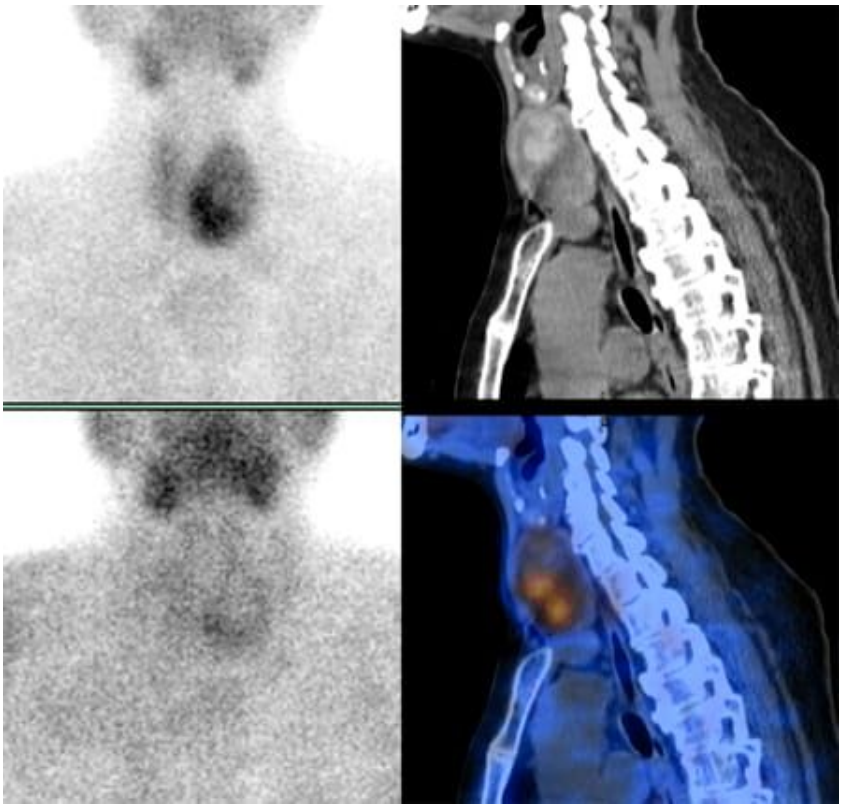

## Figure 6

A 61-year-old female patient of thyroid nodular goiter with serum Ca 2.18mmol/L and serum PTH 203.8pg/ml. Parathyroid 99mTc-MIBI SPECT/CT showed MIBI uptake lesion, which was located in the thyroid possessing mixed density with calcification.